Scaling Effects in the Compression Behavior of Sandwich Structures with Corrugated Composite Cores

J. Zhou[1], Z. Guan[1], R. Umer[2], S. Balawi[2] and W.J. Cantwell[2]

[1] School of Engineering, University of Liverpool, Liverpool, L69 3GH, U.K.

[2] Department of Aerospace Engineering, Khalifa University of Science, Technology and Research (KUSTAR), PO Box127788, Abu Dhabi, UAE.

Abstract

This project considers the mechanical properties of sandwich structures manufactured using glass fibre/epoxy and carbon fibre/epoxy curvilinear cores. The sandwich samples were produced by wrapping composite prepreg plies around Teflon-coated metal cylinders. Composite skins were then attached to the cylinders and the resulting structures were cured in a hot press. This procedure resulted in a strong bond across the skin-core interface. The resulting compression behaviour of the sandwich structures was modeled using finite element techniques.

The failure mechanisms during testing are elucidated and compared with those predicted by the FE models. The latter part of this investigation focuses on studying scaling effects in the response of both types of sandwich structure. Here, the geometry of the sandwich panels and the associated testing conditions, were adjusted appropriately to satisfy scaling laws. Following these tests, variations in compression strength and changes in failure mode are discussed.

Introduction

Sandwich structures have, for many years, been used in a great number of high-performance aerospace structures. In recent years, in an attempt to develop the next generation of lightweight structures, there has been a drive to develop sandwich structures based on novel designs, for example truss, lattice and prismatic structures [1,2]. For example, researchers have developed stretch-stretch hybrid hierarchical cores that include pyramidal lattice sandwich panels in macroscopic truss designs [4]. More recently, researchers have studied the possibility of employing corrugated composite panels in the design and manufacture of morphing structures and energy-absorbing components [3,4]. Kazemahvazi and co-workers characterized the properties of hierarchical corrugations manufactured from a carbon fibre reinforced epoxy resin [3]. The sandwich structures exhibited different failure mechanisms as the geometry of these novel structures was changed. Rejab and Cantwell [4] used a steel mould with a triangular profile to manufacture a number of corrugated cores with differing wall thicknesses and compared the resulting properties to those associated with a comparable aluminium system. It was concluded that the carbon fiber-based core offer superior properties of that of the metallic system. Malcom *et al* [5] tested a number of foam-filled and plain corrugated core structures produced from 3D glass fiber fabrics where it was shown that slender struts failed in an elastic buckling mode and thicker struts in a plastic microbuckling mechanism. Finally, Jin *et al* [6] a broad range of tests on integrated woven corrugated sandwich composites and showed that the compressive properties of these sandwich structures, offer stiffness and strength characteristics that vary with the relative density squared.

The aim of the work presented in this paper is to investigate the compressive properties of sandwich structures consisting of curvilinear composite cores. Here, the effect of varying the geometrical parameters on the compression properties of the sandwich structures is investigated. Finite element techniques are also used to explain the observed failure modes in the samples,

Excerpt from ISBN 978-3-00-053387-7

Experimental procedure

The corrugated core sandwich structure investigated in this study were prepared using a woven glass fibre reinforced plastic (GFRP), and a woven carbon fibre reinforced plastic (CFRP). The sinusoidal-shaped composite cores with varying diameter and thickness were manufactured by wrapping sheets of composite prepreg around an array of Teflon-coated steel tubes, as shown schematically in Figure 1(a). The skins of the sandwich structures were introduced by laying composite plies on the top and bottom surfaces of the uncured tubular array. Subsequently, the entire structure was cured in a hot press. Here, the panels were heated to 125 ^{o}C at a heating rate of 1.5 ^{o}C/minute. This temperature was then maintained for 90 minutes, before allowing the samples to cool to room temperature. The sandwich panels were then moved to oven and post-cured for 90 minutes at 125 ^{o}C.

In the initial part of this project, the influence of varying the corrugation diameter and thickness, on the compression strength of the cores was investigated. Here, additional steel tubes with diameters of 10, 30 and 40 mm were employed. The thickness of the corrugation was fixed at 0.5 mm for both the GFRP (four plies) and CFRP (two plies) cores. In the next part of this study, Tubes with a diameter of 20 mm were used to obtain five thicknesses of corrugation by wrapping various plies number of CFRP and GFRP, around the tubes. In the final part of this project, scaling effects in the mechanical properties of the cores were studied. Figure 1(b) shows photographs of the four scale sizes of CFRP sandwich panel. As before, each sample was based on two unit cells. Here, steel tubes with diameters of 40n mm were used, where n is the scale size, taken as ¼, ½, ¾ and 1 in this investigation. The thickness of the core corrugation and the skins in each panel were also varied in order to ensure that scaling laws were respected. The width and length of the test samples were 40n mm and 160n mm respectively.

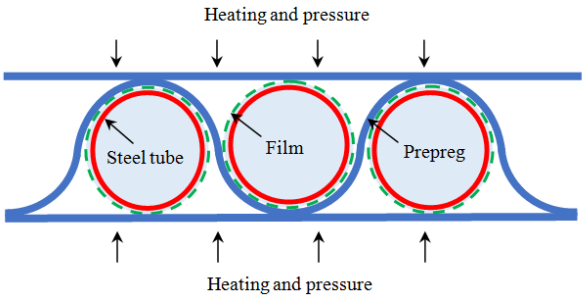

(a) Schematic of the corrugated core sandwich structure.

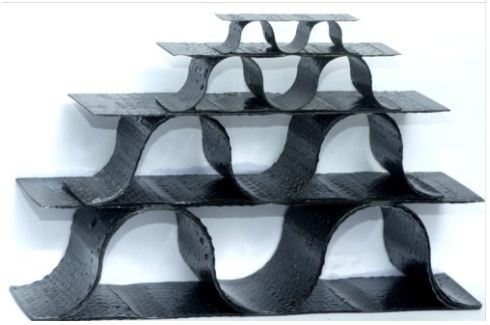

(b) Four scaled sizes of CFRP core (n=1/4, n=1/2, n=3/4 and n=1).

Figure 1. Schematic and photographs of the corrugated core sandwich structure.

Compression tests were undertaken at a crosshead displacement rate of 1 mm/min using a universal Instron 4045 test machine. In this case of the scaled sandwich structures, a crosshead displacement rate of 4n mm/min was employed during testing. Potential changes in failure mode were photographed at regular intervals during testing in order to elucidate the modes of failure and fracture.

Excerpt from ISBN 978-3-00-053387-7

Finite Element Modelling

Finite element models were created to model the compression response of the sandwich structures under quasi-static loading. Here, the cores were meshed using eight-noded (C3D8R) solid elements with reduced integration. A mesh size of 1 x 1 mm within the plane and two elements through-thickness of composite layers were used in this study. The composite was modeled using modified Hashin's 3D failure criteria. The user-defined 3D failure criteria [7, 8] were used to simulate the response of these materials in the Cartesian coordinate system (x, *y*, z). The failure criteria, together with the related constitutive model, were then implemented into the ABAQUS/Explicit [9].

Results and Discussion

The Influence of Corrugation Diameter

Figure 2a shows load-displacement traces following tests on the glass-based system with values of d between 10 and 40 mm. The planar sizes of these samples were 400 mm^2 for the 10 mm sample and 6400 m^2 for the 40 mm diameter specimens. All four traces exhibit similar trends, with the force increasing to a maximum before dropping sharply. Increasing the value of 'd' leads to greater levels of non-linearity in the initial slope and a reduction in the maximum load. In all cases, the load begins to increase rapidly during the later stages of the test, typically when the nominal strain has exceeded 60%. Figure 2b shows the variation of compression strength with 'd' for both the glass and carbon-based materials. The figure clearly shows that the strength decreases rapidly with increasing 'd', with the CFRP panels outperforming the glass systems.

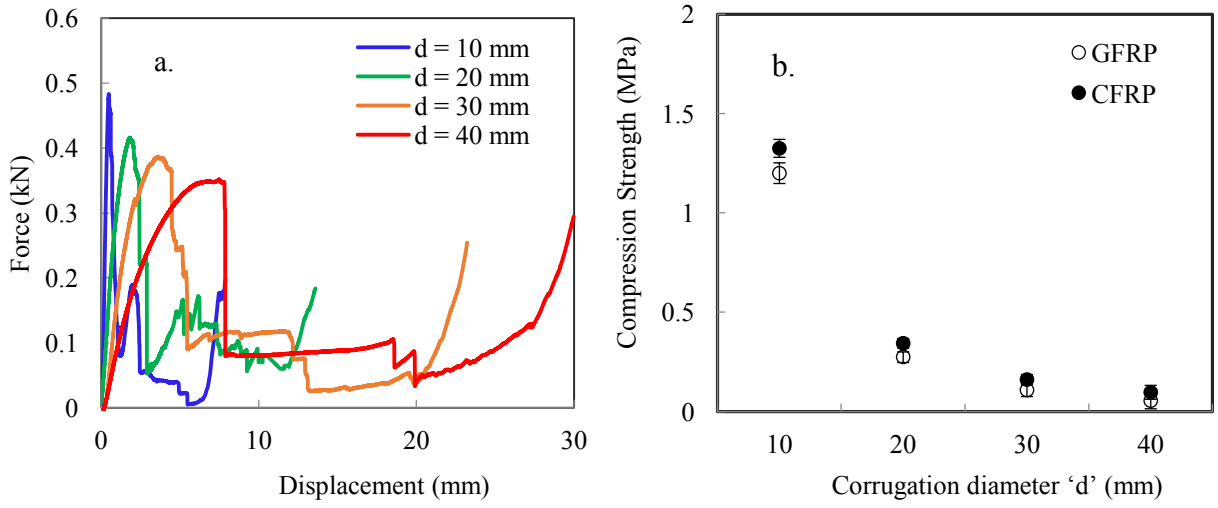

Figure 2. The influence of corrugation diameter 'd' on the compression properties of GFRP samples with a corrugation thickness of 0.5 mm.

The Influence of Corrugation Thickness

Figure 3 presents typical stress-strain traces following compression tests on GFRP and CFRP samples with corrugation thicknesses 't' between 0.25 and 1.25 mm. An examination of the response of those structures, Figure 3(a), indicates that increasing the value of 't' serves to increase the compression strength of the core. The strength of the thinnest core is clearly very low, reaching a value 0.1 MPa before dropping to a value close to zero.

Excerpt from ISBN 978-3-00-053387-7

As expected, increasing the value of 't' to 0.5 mm results in a similar load-displacement, with the maximum value reaching 0.3 MPa, before dropping to a lower value, as the core buckled under continued compressive loading. Further increases in thickness precipitated a change in the shape of the stress-strain trace, with the curves exhibiting several peaks before the onset of final densification. This is most pronounced in the thickest sample, where the stress initially increases to 2.0 MPa before reducing and then increasing a second time to 1.6 MPa and finally to a peak at 0.5 MPa prior to the onset of densification.

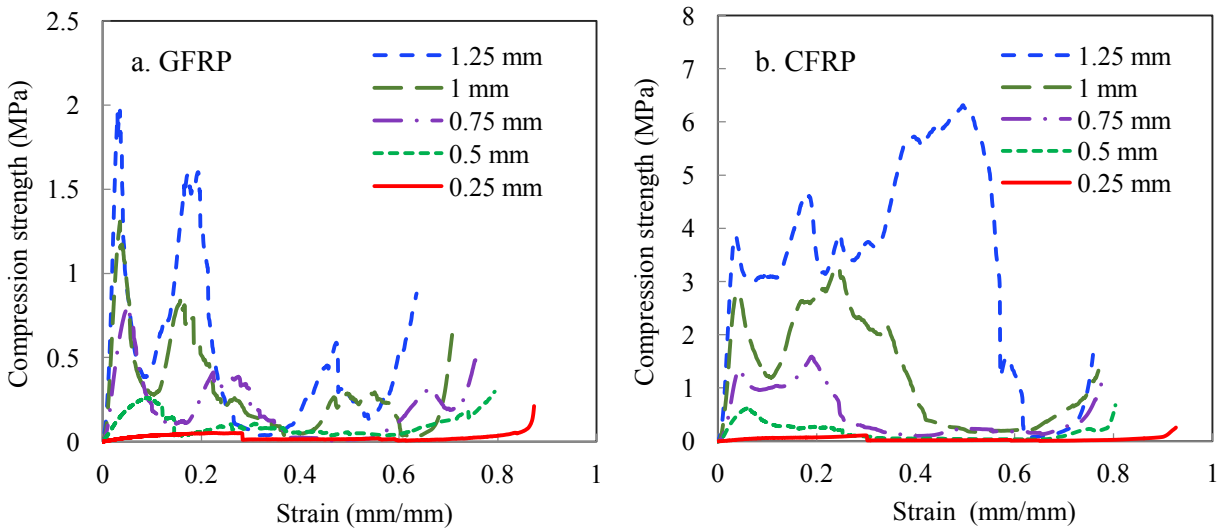

Figure 3. Compression stress-strain traces for GFRP and CFRP samples based on various corrugation thicknesses.

Figure 3(b) shows stress-strain curves for the carbon fiber core. It is encouraging to note that the CFRP cores, in most cases, are much stronger than their GFRP counterparts. However, as before, similar trends to those observed samples based on thin walls fail at very low stresses, exhibiting a single peak prior to failure. Increasing the thickness of the wall to 0.75 mm resulted in the trace exhibiting two peaks before complete failure. Similarly, the 1.0 mm thick sample exhibits two distinct peaks and the thickest specimen exhibits a number of increasing peaks prior to failure at a strain of approximately 0.6.

Figure 4 shows comparison between experimental observations and FE prediction of the failure modes in CFRP samples with web thicknesses of 0.25, 0.75 and 1.25 mm. Generally good agreement between experimental observations and the predictions shown in the figure, with the model predicting flattening of the core against the surface skins, buckling in the walls of the core as well as localized creasing of the composite. Initial deformation in the 0.25 mm thick samples is associated with the flattening of the webs against the lower and upper skins, followed by buckling of one side of the unit cell. This deformation mechanism leads to creasing and fracture of the corrugation. Failure in the 0.75 mm thick samples involved initial buckling and creasing close to the upper skin, followed by a buckling failure of the webs at their mid-points. This two stage process resulted in the two peaks observed in the loading trace. Finally, failure in the 1.25 mm thick samples involved the formation of a clear 90 degree hinge at the vertical alignment of the webs and the top surface. These re-aligned webs were capable of supporting significant load before failing, leading to the second distinct peak in the stress-strain trace.

Excerpt from ISBN 978-3-00-053387-7

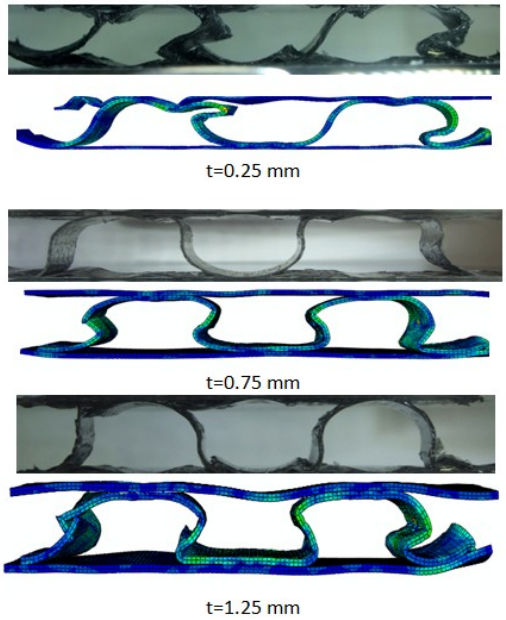

Figure 4. Comparison failure of CFRP samples based on an increasing wall thickness between FE and test.

Figure 5(a) summarized the results of the compression tests on the GFRP and CFRP cores are. It is clear that the compression strength increases in a non-linear fashion as 't' increases. For example, increasing the corrugation thickness from 0.25 to 1.25 mm results in a sixty-seven fold increase in the compression strength of the GFRP samples. The corresponding increase is even greater for the CFRP samples. the carbon fibre-based core out-performs its glass fibre counterpart, with the difference in strength increasing as the corrugation thickness 't' is increased. It is worth noting that the densities of the CFRP cores were lower for a given value of 't', suggesting that the relative performance of the carbon fibre systems is even more impressive than that shown in the figure.

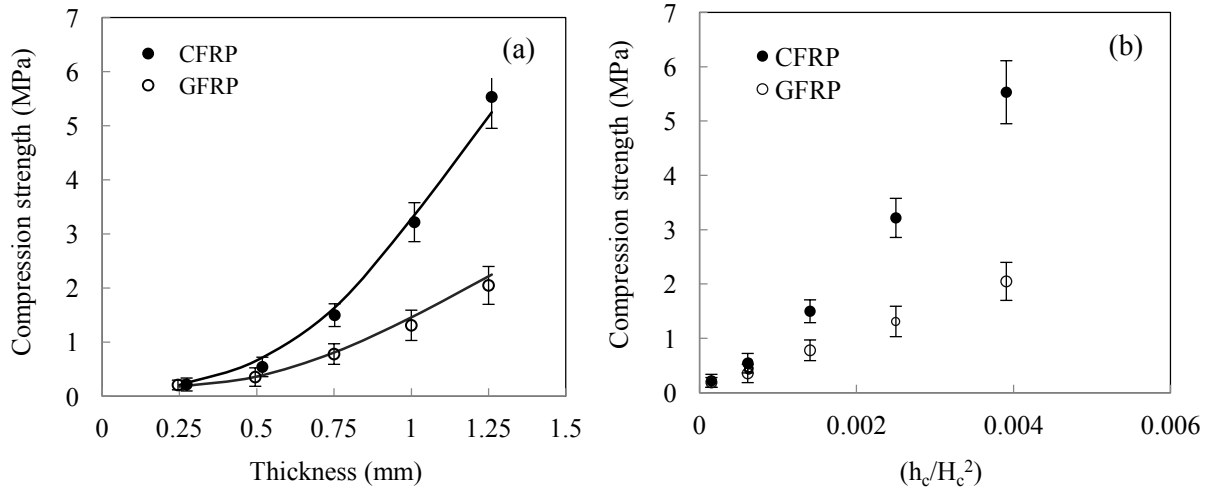

Figure 5. The variation of compression strength versus thickness and $(h_c/H_c)^2$ for GFRP and CFRP samples based on 20 mm diameter. (a) Corrugation thickness of the corrugation. The solid lines correspond to the FE predictions. (b) The corrugated cores with $(h_c/H_c)^2$.

Malcom, *et al* [5] investigated these trends in compression strength with corrugation thickness mirror those observed following compression tests on corrugated core materials. Jin *et al* [6] stated that the compression strength of corrugated composite structures varied with the square of the relative density of the core. Zhang *et al* [10] studied

Excerpt from ISBN 978-3-00-053387-7

the compression response of sinusoidal corrugated structures based on stainless steel and developed an analytical solution to simulate failure through the formation of plastic hinges. Similarly, those studies showed that the normal compression strength of the core varies with the yield strength of the base material according to the square of (h_c/H_c) where h_c is the thickness of the corrugation and H_c the height of the core. Figure 5(b) presents plots of compression strength versus the square of (h_c/H_c) for both types of core. It is evident that the compression properties appear to loosely follow a relationship based on the square of h_c/H_c for a given material system. Differences in the slopes of the two traces reflect distinct differences in mechanical properties of the two types of composite.

Scaling Effects in the Compressive Properties of the Cores

The effect of varying the specimen size on the compressive properties of the GFRP and CFRP cores was assessed by undertaking tests on the GFRP and CFRP. The compressive tests were undertaken at a constant scaled crosshead displacement rate of 4n mm/minute. Typical load-displacement traces following compression tests on the four scaled sizes of GFRP core are shown in Figure 6(a). An examination of the figure indicates that all four traces exhibit similar trends, with the four curves increasing to a maximum before reaching a peak and subsequently dropping sharply. Continued loading of the four samples results in an intermediate loading regime, wherein failure of the cores occurs at relatively low levels of force. The load-displacement traces for the GFRP samples were then normalised whereby the force was divided by the square of the scale size (i.e. n^2) and the displacement by the scale size, n. The resulting normalised traces for these glass-based samples are shown in Figure 6(b). From the figure, it indicates that the four curves appear to collapse onto a relatively unique trace. The maximum force values as well as the densification thresholds are similar for all four samples. An examination of this figure evident that the compression properties of these GFRP samples obey a simples scaling law suggesting that such an approach can be employed to predict the response of larger structures.

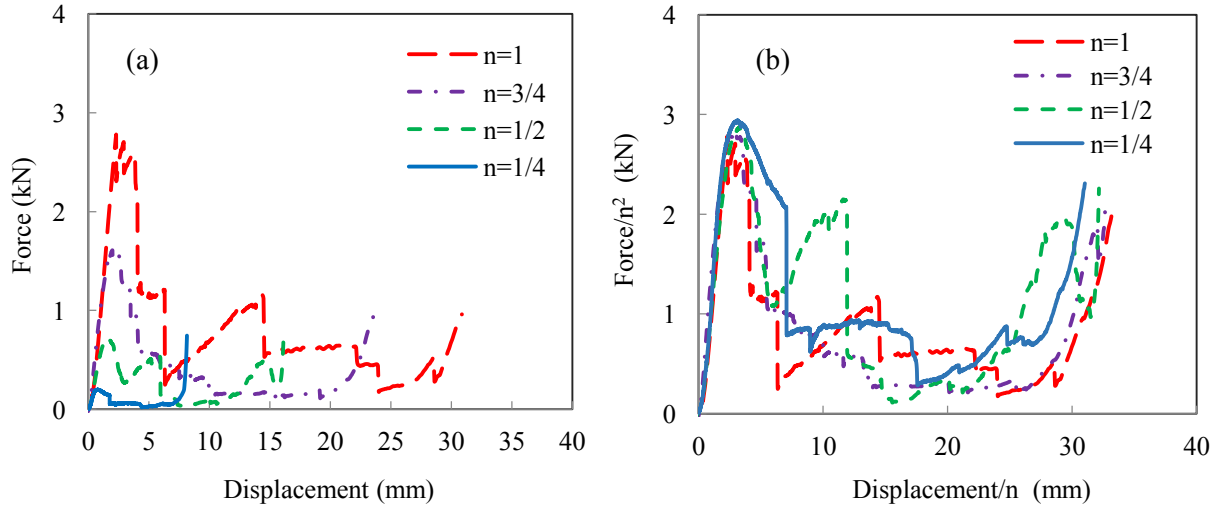

Figure 6. Compression tests on the GFRP samples (a) original force-displacement traces (b) scaled force-displacement traces.

The influence of scale size on the compression strength of the curvilinear cores was summarized in Figure 7. An inspection of the figure highlights an absence of any appreciable size effect in the compressive properties of the glass fibre-based material. Here, the compression strength of the GFRP core is roughly constant over the range of specimen sizes, with the strength averaging approximately 0.45 MPa. In contrast, the compression strength of the carbon based cores increases slightly with scale size. Given that the n = ¼ CFRP system is only based on one ply and the height of the core is just over ten times the length of the weave, local variations in the weave characteristics are likely to be much greater in the smallest sample than for the case where n = 1, in which there are four plies with

Excerpt from ISBN 978-3-00-053387-7

a core height that is approximately 55 times that of the weave size. Figure 7 indicates that scaling techniques can be used to obtain an initial estimation of the response of larger, more-representative structures.

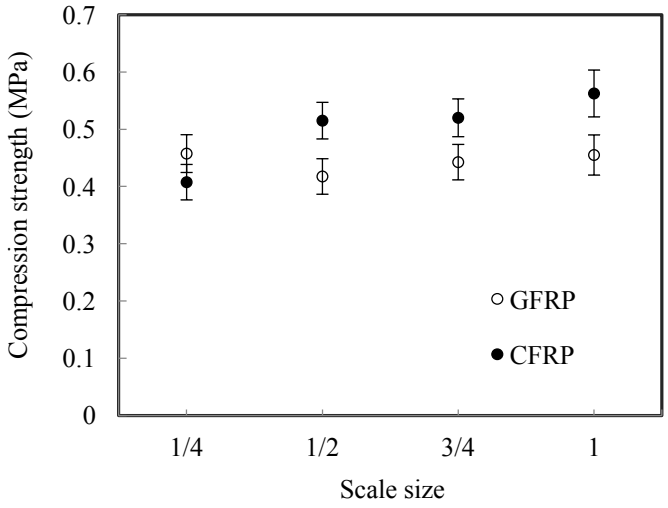

Figure 7. Compression strength versus scale size for scaled GFRP and CFRP samples following testing at a crosshead displacement rate of 4n mm/minute. The lines correspond to the FE predictions.

Excerpt from ISBN 978-3-00-053387-7

Conclusions

The mechanical response of all-composite sandwich structures have been investigated experimental and numerically. The compressive response of the sandwich structures was predicted accurately using the developed finite element model, successfully predicting the observed failure mode in most cases. A range of sandwich structures based on corrugated core have been manufactured by compression molding an array of wrapped metallic cylinders. Tests on the resulting samples indicated that the compression strength decreased with the diameter of the corrugation. The stress-strain traces for the thicker samples exhibited more than one peak, failure mechanisms that were associated with buckling of the web, the formation of a hinge and the re-orienting of the individual webs. It is indicates that the carbon fiber reinforced corrugated structures offered superior compressive properties to its glass-based counterpart. It also clear that compression strength increased rapidly with the thickness of the corrugation. The final part of this study focused on investigating the scaling response of the glass and carbon/epoxy structures. All four load-displacement curves collapsing onto a relatively unique trace following the normalization process and there was no significant scaling effects were observed in the four scaled sizes. This study suggests that the mechanical response of more representative sandwich structures can be predicted accurately by using a simple scaling approach.

References

[1]. J. Xiong, B. Wang, L. Ma, J. Papadopoulos, A. Vaziri and L. Wu, Three-dimensional composite lattice structures fabricated by electrical discharge machining: Experimental mechanics 2013;54:405–412.
[2]. S. Yin, L. Wu and S. R. Nutt, Compressive efficiency of stretch-stretch-hybrid hierarchical composite lattice cores. Materials and Design 2014; 56:731–739.
[3]. S. Kazemahvazi, D. Tanner and D. Zenkert, Corrugated all-composite sandwich structures. Part 2: Failure mechanisms and experimental programme. Composites Science and Technology 2009;69:920-925.
[4]. M. R. M. Rejab and W. J. Cantwell, The mechanical behaviour of corrugated-core sandwich panels. Composites. Part B Engineering 2013;47:267–277.
[5]. A.J. Malcom, M.T. Aronson, V.S. Deshpande and N.H.G. Wadley, Compressive response of glass fiber composite sandwich structures. Composites Part A – Applied Science and Manufacturing 2013;54:88-97.
[6]. F.N. Jin, H.L. Chen, L. Zhao, H.L. Fan, C.G. Cai and N. Kuang, Failure mechanisms of sandwich composites with orthotropic integrated woven corrugated cores: Experiments. Composite Structures 2013;98: 53-58.
[7]. Z. Hashin, Failure criteria for unidirectional fiber composites. Journal of Applied Mechanics 1980;47:329-334.
[8]. E. Sitnikova, Z.W. Guan, G.K. Schleyer, W.J.Cantwell, Modelling of perforation failure in fibre metal laminates subjected to high impulsive blast loading. International Journal of Solids and Structures 2014; 51: 3135-3146.
[9]. T. P. Vo, Z. W. Guan, W. J. Cantwell, G. K. Schleyer. Modelling of the low-impulse blast behaviour of fibre–metal laminates based on different aluminium alloys. Composites: Part B 2013;44: 141–151.
[10]. J. X. Zhang, Q. H. Qin and T. J. Wang, Compressive strengths and dynamic response of corrugated metal sandwich plates with unfilled and foam-filled sinusoidal plate cores. Acta Mechanica 2013;224:759–775.

Excerpt from ISBN 978-3-00-053387-7